REPRINTS

ELSEVIER

Thin Solid Films 307 (1997) 221–227

thin solid films

Preparation and study of doped and undoped tin dioxide films by the open air chemical vapour deposition technique

Sekhar C. Ray, Malay K. Karanjai, Dhruba Dasgupta *

Department of Physics, University of North Bengal, Siliguri, Darjeeling 734430, West Bengal, India

Received 11 September 1996; accepted 30 April 1997

Abstract

Highly transparent and conducting undoped and doped (Mo, Sb, F) tin dioxide films have been prepared by the open air chemical vapour deposition technique. The electrical and optical properties have been studied in detail for films deposited on glass substrates. Surface morphology study by scanning electron microscope shows that for films deposited on glass substrates, Sb- and F-doped films have a larger grain size than undoped ones. Mo-doping, in contrast, produces smaller grains. Films deposited on mica and Al sheet substrate have also a larger grain size compared to those on glass substrate. Films of very high quality in terms of crystallinity, electrical conductivity and optical transmission were obtained when deposited at a substrate temperature of 400°C. The optimum concentration for each dopant, at which the sheet resistance is a minimum, has been determined. 4.5 at.% F-doped SnO_2 films show the lowest resistivity, $\sim 4 \times 10^{-4}$ Ω cm, and an average optical transmission of 80% at a thickness of 3500 Å. © 1997 Elsevier Science S.A.

Keywords: Transparent conducting oxide; SnO_2 thin films; CVD

1. Introduction

Tin dioxide has been widely used as a transparent conducting thin film material for application in a number of solid state devices such as solar cells, opto-electronic devices, liquid crystal displays, heat mirrors, photo-thermal converters, thin film resistors and gas sensors [1–4].

The films are also very useful because of the stability of their mechanical, optical and electrical properties. Tin dioxide is a wide band gap electron degenerate semiconductor, whose properties largely depend on the deviation from stoichiometry (oxygen deficiency) as well as on the dopants used. Usually antimony or fluorine is used as a dopant to substitute tin or oxygen atoms, respectively.

Tin dioxide films have been prepared by a large variety of techniques which include spray pyrolysis [5–12], chemical vapour deposition [13–17], sol-gel method [18–20], reactive evaporation [21] and reactive r.f. sputtering [22]. The properties of these films crucially depend on the deposition technique and post deposition treatment.

In a previous report [23] we described an extremely simple and low-cost chemical vapour deposition method for tin dioxide films. In this method, the starting material is $SnCl_2 \cdot 2H_2O$ crystals which are ground with water into a paste and the paste applied in the form of a 4–5 mm wide band near, and parallel to, the lower edge of a substrate positioned vertically. On heating in air the paste decomposes according to the equation

$$6SnCl_2 + H_2O \rightarrow 2SnCl_4 + 4Sn(OH)Cl.$$

$SnCl_4$, which is generated as one of the reaction products, rises upward due to convection and hydrolyses on the heated substrate to produce a tin dioxide film. Doping with antimony can be achieved by mixing the requisite amount of $SbCl_3$ with $SnCl_2$ paste. Considering the simplicity of the method, films of reasonably good quality can be obtained. Details are given in Ref. [23].

This so-called 'paste-heat' method, however, suffers from the following disadvantages: (i) the portion of the substrate where the $SnCl_2$ paste is applied must be subsequently cut away before the films can be used, (ii) because of the geometry of the arrangement, the films are non-uniform, being thickest near the paste-coated area and becoming thinner away from it, and (iii) non-planar substrates, as also those with small sizes cannot be used.

* Corresponding author. Tel.: +91 353 450414; fax: +91 353 450546; e-mail: dhruba@nbu.ernet.in

PII S0040-6090(97)00268-X

In this report, we describe a modification of the above method, which employs the same principle, and maintains essentially the same simplicity, at the same time enabling one to obtain films free from the above defects. The preparation of undoped and doped (Sb, Mo, F) tin dioxide thin films by this method and the study of their electrical and optical properties as well as their surface morphology and crystal structure are described.

2. Experimental details

A 75 cm long glass tube with an internal diameter of 5 cm was placed vertically as shown in Fig. 1. The tube was heated from the outside in atmospheric condition by winding a heater coil on its outer surface over a length of 70 cm. The substrate was placed vertically in the central region of the tube. The starting material was taken in a conical flask placed at the bottom of the tube and heated separately. The temperature of the substrate was measured by a thermocouple placed close to the substrate. The starting material was prepared by mixing crystals of $SnCl_2$, $2H_2O$ with a few drops of water along with any dopant material that might be added and was stirred mechanically to convert it to a paste.

In the film forming process, the substrate was initially heated to attain the desired temperature after which the $SnCl_2$ paste was heated. White fumes were given off by the paste and were seen to deposit SnO_2 films where they came into contact with the hot substrate.

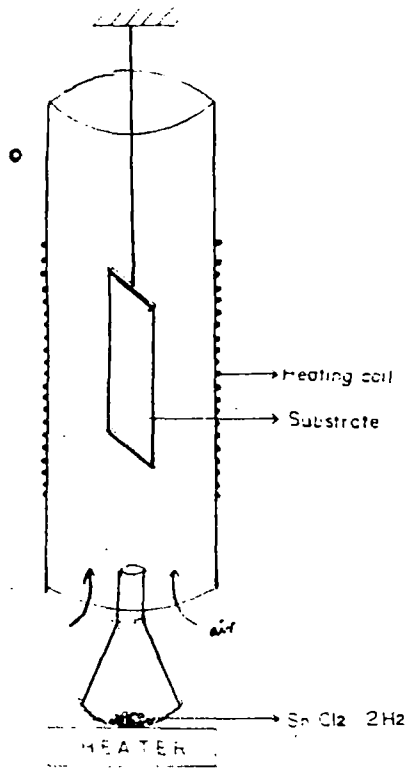

Fig. 1. Experimental arrangement for the deposition of SnO_2 films.

It is possible to deposit a number of films in a batch, by attaching them to a holder, which is placed in the central region of the tube. Usually both sides of the substrate are coated by this method, which is advantageous in some special cases [24], but it is also possible to coat one side only by masking the other side, or by fixing two substrates back to back. This method is especially advantageous for inaccessible surfaces and the inside surface of a tube, where one can obtain a coating quite easily, in contrast to the rather complex arrangements required in the usual CVD methods. The films were usually deposited over soda glass substrates (7.5 cm × 2.5 cm) and showed a uniform interference colour over their entire area except at the edges. But uniform films could also be routinely obtained, if necessary, over a larger area of 40 cm long by 4 cm wide.

Undoped tin dioxide films of various thicknesses were prepared at substrate temperatures of 350°C, 400°C and 450°C. Soda glass microslides, mica and Al sheet were used as substrates.

The films were doped with antimony, fluorine and molybdenum by adding antimony trichloride, ammonium fluoride and ammonium molybdate respectively to the $SnCl_2$ starting material. Characterization of the films was carried out by optical transmission and electrical conductivity measurements, X-ray diffractometry and scanning electron microscopy.

The electrical properties of the films were measured by the standard four-probe method and the optical properties were studied by a Shimadzu UV-240 double-beam spectrophotometer. Surface morphology and X-ray diffractometric studies were carried out by a Hitachi S-530 scanning electron microscope and a Philips diffractometer (model PW 1390) with CuK_α radiation (Ni-filter) at 1.54 Å, respectively.

3. Results and discussions

The films were smooth, highly uniform and resistant to peeling-off and acids, and also showed long-term stability with respect to their optical, electrical and mechanical properties. They displayed characteristic interference colours. Films of various thicknesses were obtained by varying the amount of starting material, deposition time and substrate temperature. By observing the change in interference colours as a function of time the order of a particular colour could be known, and from the standard value of the mean refractive index of SnO_2 (taken as 2.0 over the range of 400–800 nm) the thickness could be estimated [25].

It was found that using this process a substrate temperature of 400°C was necessary to prepare films of very high quality in terms of conductivity, optical transmission, uni-

formity and resistance to peeling-off and acids as well as environmental shocks.

3.1. X-ray diffractometric study

X-ray diffractometric studies were carried out on undoped and doped SnO_2 films deposited at a substrate temperature of 400°C. Diffraction peaks for undoped SnO_2 films having two different thicknesses are shown in Fig. 2(a). Fig. 2(b) shows the X-ray diffractograms of Sb and F doped SnO_2 films. The crystal structure is in accordance with the usual tetragonal form of SnO_2.

It is clear from the XRD patterns that there is no amorphous background in the diffractograms of the deposited films. Moreover, none of the undoped films show any preferred orientation, while those doped with Sb and F show a preferred orientation along the (110) planes. Prominent peaks, their d-values and relative intensities (I/I_0) for a typical F-doped SnO_2 film are listed in Table 1.

3.2. Surface morphology

Surface topographies of undoped, 6 at.% Mo-doped, 1.5 at.% Sb-doped, and 4.5 at.% F-doped SnO_2 films de-

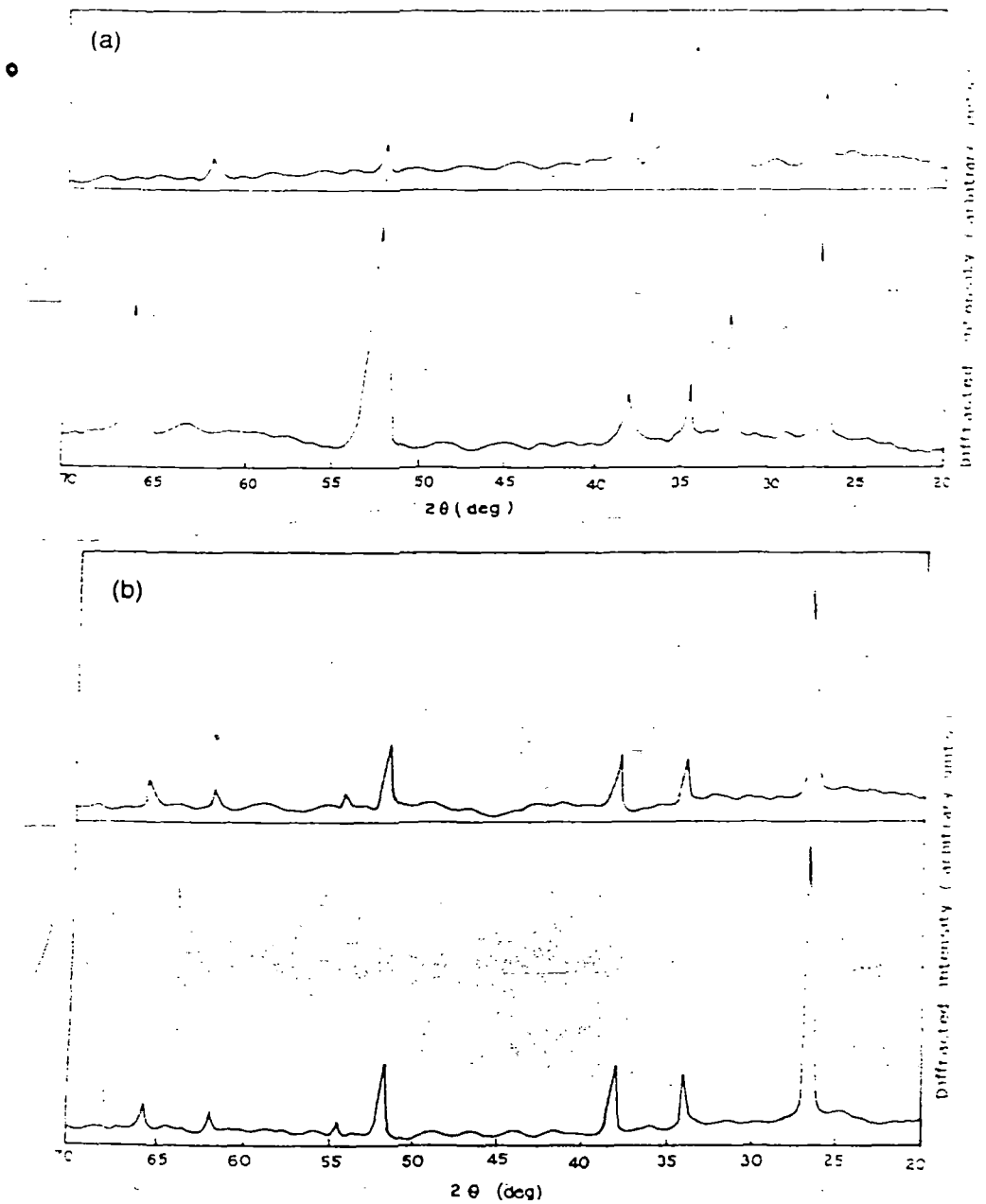

Fig. 2. (a) X-ray diffractogram of undoped SnO_2 films of two different thicknesses (T_s = 400°C). (i) 0.6 μm (ii) 2.5 μm. (b) X-ray diffractogram of doped films (T_s = 400°C). (i) 1.5 at.% Sb-doped. (ii) 4.5 at.% F-doped.

Table 1
Prominent peak positions (2θ values) of the X-ray diffraction peaks, corresponding d-values, relative intensities (I/I_0) and their identification for F-doped SnO_2 films

Observed values			Comparable values from ASTM data file			
2θ	d-value [Å]	(I/I_0)	2θ	d-values [Å]	(I/I_0)	hkl
26.60	3.347	100	26.57	3.351	100	110
33.90	2.641	21	33.86	2.644	80	101
37.95	2.368	32	37.94	2.369	25	200
51.75	1.764	34	51.73	1.765	65	211
54.85	1.671	12	54.74	1.675	18	220
61.95	1.496	12	61.86	1.498	14	310
65.90	1.415	13	65.94	1.415	16	301

posited at a substrate temperature of 400°C are shown in Fig. 3. It is observed that in all cases except that of Mo-doped films large size grains of ~ 1.7 μm are spread throughout the film over a background of grain size ~ 0.6 μm. These large grains are observed to disappear when doped with Mo. The average grain size for Sb- and F-doped films is found to be larger, while that for Mo-doped films is smaller compared to the undoped ones.

Films were also deposited on different substrates to investigate the substrate effect. Fig. 4 shows the SEM micrographs of undoped SnO_2 films deposited on mica and aluminium sheet at a substrate temperature of 400°C. It is also evident from Fig. 4 that the grain size of the undoped SnO_2 films deposited on crystalline mica and aluminium substrate is larger than that deposited on glass substrates. Table 2 shows the grain size variation of the films deposited.

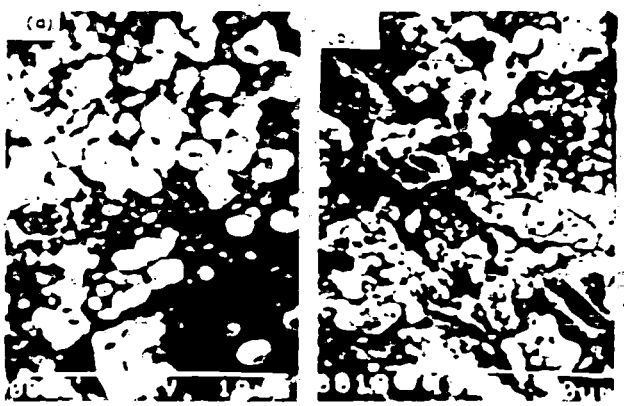

Fig. 4. Scanning electron micrographs of SnO_2 thin films on different substrates (T_s = 400°C). (a) On mica, (b) on aluminium sheet.

3.3. Electrical properties

Results of detailed measurements of the sheet resistance of the films as a function of thickness, temperature and dopant concentration are shown in Figs. 5 and 6.

Fig. 5 shows the variation of sheet resistance with thickness of undoped films deposited at three substrate temperatures. It is evident from the curves that the room temperature resistivity of the undoped films decreases to its minimum value when deposited at a substrate temperature of 400°C but increases again when deposited at a higher substrate temperature of 450°C. This is due to the fact that, on increasing the substrate temperature from 350°C to 400°C, a better degree of crystallinity is achieved, leading to improved electronic, optical and structural properties [8,26]. It is also known that [5] both the carrier

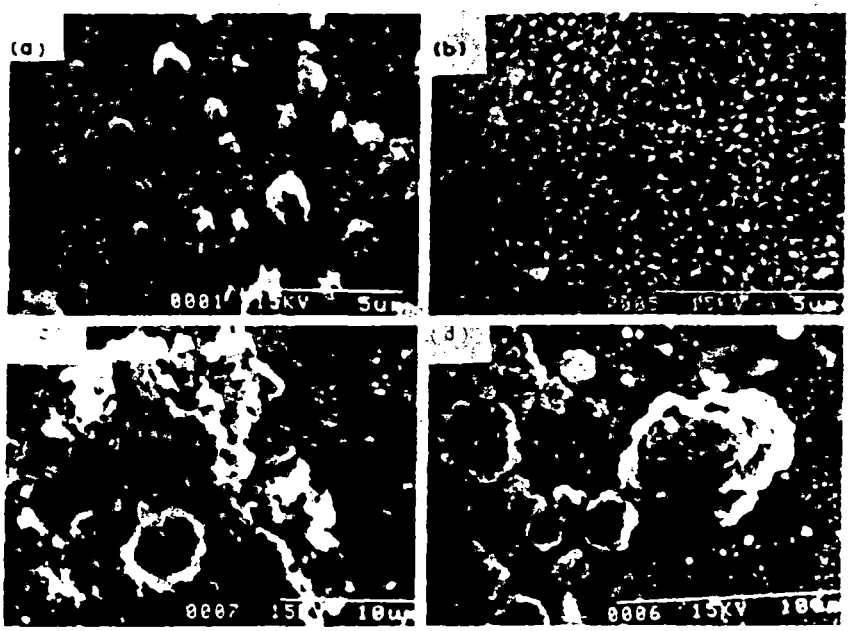

Fig. 3. Scanning electron micrographs of SnO_2 thin films on glass substrates (T_s = 400°C). (a) Undoped SnO_2; (b) SnO_2:Mo (6 at.%); (c) SnO_2:Sb (1.5 at.%); (d) SnO_2:F (4.5at.%).

Table 2
Grain size variation of doped (on glass) and undoped (on different substrates) SnO_2 films (deposition temperature T_s = 400°C)

Films	Substrate	Average grain size [μm]
SnO_2 undoped	glass	1.20
SnO_2:Sb	glass	4.00
SnO_2:Mo	glass	0.60
SnO_2:F	glass	4.75
SnO_2 undoped	mica	2.00
SnO_2 undoped	aluminium	1.50

concentration and mobility increase with the increase of substrate temperature where mobility variation is larger than that of the carrier concentration. A further increase in substrate temperature produces films of increased resistivity. This is due to the fact that in undoped SnO_2, conduction electrons arise from oxygen vacancies, and a higher substrate temperature causes an increased oxygen evolution from the substrate, leading to more nearly stoichiometric films [8,27]. The resistivity of the undoped films prepared at a substrate temperature of 400°C is estimated to be 4×10^{-3} Ω cm, which agrees well with the values reported earlier in the literature [8].

The effect of dopants (Mo, Sb, and F) at various concentrations on the resistivity was studied. It is found that for every dopant, there is an optimum concentration at which the resistivity is a minimum. These values are listed in Table 3.

Thus it is observed that the introduction of Mo reduces the resistivity by a maximum factor of 2 whereas Sb and F reduce it by factors of 5 and 10, respectively. Similar results are reported by Gordillo et al. [7]. The relatively

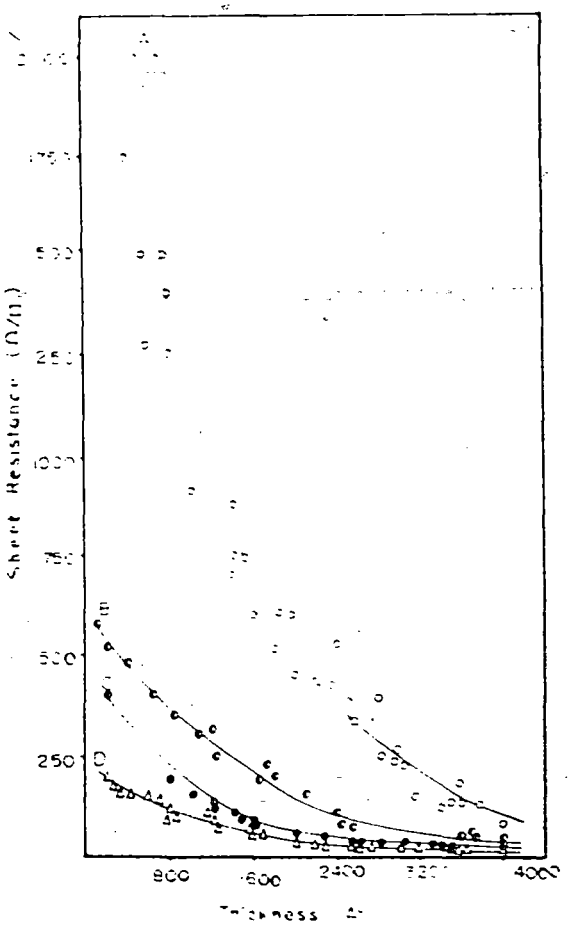

Fig. 6. Sheet resistance–thickness relationship for undoped (curve A) and doped (curve B, SnO_2:Mo (6 at.%); curve C, SnO_2:Sb (1.5 at.%); curve D, SnO_2:F (4.5 at.%)) SnO_2 films prepared at a substrate temperature of 400°C.

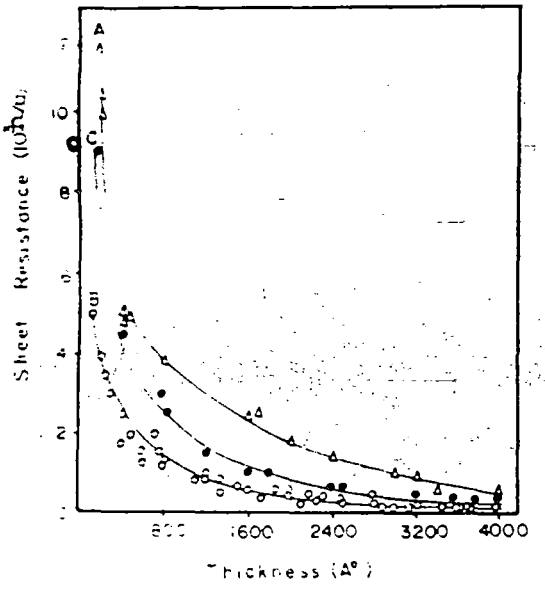

Fig. 5. Variation of sheet resistance with thickness of undoped SnO_2 films deposited at various substrate temperatures. A, 350°C; B, 400°C; C, 450°C.

higher resistivity and lower optical transmission of the Mo-doped SnO_2 films compared to the Sb-doped and F-doped films may be due to their small grain size as observed from the SEM micrograph. It is known that with the decrease in grain size the grain boundary potential increases, leading to an increased grain boundary scattering and a corresponding increase in resistivity [5]. In the case of Sb-doped and F-doped SnO_2 films, the resistivity decreases up to 1.5 at.% Sb-doping and 4.5 at.% F-doping, respectively, which may be due to (i) increased carrier concentration, (ii) larger grain size and (iii) preferred orientation. Beyond the above concentration the observed

Table 3
Minimum resistivity values of undoped and doped SnO_2 films on glass substrate (T_s = 400°C)

Films	Resistivity [Ω cm]
SnO_2 (undoped)	4×10^{-3}
SnO_2:Mo (6 at.%)	2×10^{-3}
SnO_2:Sb (1.5 at.%)	8×10^{-4}
SnO_2:F (4.5 at.%)	4×10^{-4}

increases in resistivity may be due to the increase in the contribution from ionised impurity scattering [5].

The variation of sheet resistance with thickness for optimum concentrations of the dopants is shown in Fig. 6.

3.4 Optical properties

The variation of the average optical transmission over the range 400–800 nm as a function of sheet resistance for undoped and doped films is shown in Fig. 7. The optical transmission is observed to decrease with decreasing sheet resistance in the case of both undoped and doped films. It is seen for all the films that the optical transmission drops off more rapidly at lower values of the sheet resistance. This is due to an increase in surface roughness of films having a low sheet resistance which have a proportionately higher thickness [1,26]. However, F-doped films are found to have a high optical transmission even at a low sheet resistance of 100 Ω/□.

The films are found to compare quite favourably in terms of electrical and optical properties with those prepared by other methods as shown in Table 4. The figure of merit ϕ_{TC} for the films has been calculated according to Haäcke's [28] relation $\phi_{TC} = T^{10}/R_s$ for transparent conducting films, where T is the transmission and R_s the sheet resistance.

3.5. Conclusions

Undoped and Mo-, Sb-, and F-doped SnO_2 films deposited by the Open Air Chemical Vapour Deposition (OACVD) technique have been investigated in detail. The films show a high degree of crystallinity along with the largest values of electrical conductivity and optical transmission when deposited at a substrate temperature of 400°C. X-ray diffractometric study suggests that Sb- and F-doped SnO_2 films show a preferred orientation along the (110) plane. The surface morphology study by scanning

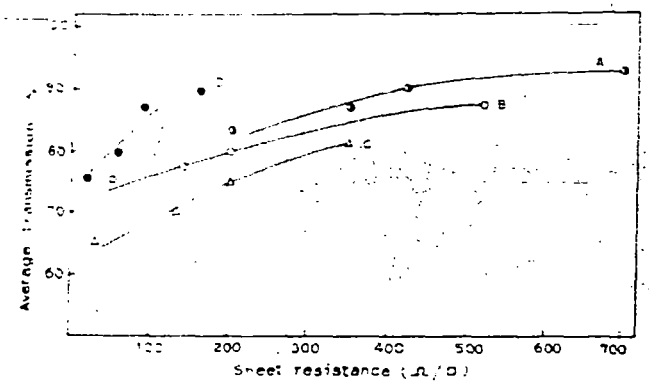

Fig. 7. The average optical transmission over 400–800 nm versus sheet resistance for undoped (curve A) and doped (curve B, SnO_2:Mo (6 at.%); curve C, SnO_2:Sb (1.5 at.%); curve D, SnO_2:F (4.5 at.%)) SnO_2 films prepared at a substrate temperature of 400°C.

Table 4
Comparison of the electrical and optical properties of tin dioxide films prepared by various workers

Material	Deposition technique	ρ	R_s	$T_a(\Delta\lambda)$	ϕ_{TC}
SnO_2	SP [27]	5×10^{-3}	83	85 (0.5–2)	2.40
	CVD [29]	7×10^{-3}	1200	93 (0.5–0.7)	0.42
	present work	4×10^{-3}	100	90 (0.4–0.8)	3.48
SnO_2:Sb	SP [1]	4.2×10^{-3}	28	87 (0.3–1)	9.40
	CVD [30]	2×10^{-3}	55	88 (0.4–0.7)	5.06
	present work	8×10^{-4}	20	75 (0.4–0.8)	2.82
SnO_2:F	SP [1]	4.6×10^{-3}	10	85 (0.4–1)	19.68
	CVD [13]	5×10^{-4}	20	90 (0.4–0.8)	17.43
	present work	4×10^{-4}	10	85 (0.4–0.8)	19.68
SnO_2:Mo	present work	2×10^{-3}	50	80 (0.4–0.8)	2.15

ρ = resistivity [Ω cm], R_s = sheet resistance [Ω □], $T_a(\Delta\lambda)$ = average optical transmission (wavelength range [%] (μm)), ϕ_{TC} = figure of merit [$\times 10^{-3}$ Ω^{-1}], CVD = chemical vapour deposition, SP = spray pyrolysis.

electron microscope suggests that for films deposited on glass substrates, the grain size increases in the case of Sb-doped and F-doped SnO_2 films but decreases for Mo-doped SnO_2 films. The grain size for undoped films on mica and aluminium sheet substrate is also larger than that for films deposited on glass substrates.

The lowest values of sheet resistance at a particular thickness are obtained for 6 at.% Mo-doped, 1.5 at.% Sb-doped and 4.5 at.% F-doped SnO_2 films on glass substrate. A typical value of resistivity of 4.5 at.% F-doped SnO_2 films is 4×10^{-4} Ω cm and that for 1.5 at.% Sb-doped SnO_2 is $\sim 8 \times 10^{-4}$ Ω cm.

The films compare quite well in terms of electrical conductivity and optical transmission with those obtained by other methods. The average optical transmission over the range of 400 to 800 nm is found to decrease as the sheet resistance decreases for Mo- and Sb-doped films. But for F-doped films, a negligible increase in transmission loss with decreasing sheet resistance is found to occur.

In conclusion, tin dioxide films having a sheet resistance of 10–1000 Ω/□ and an average optical transmission of 75–90% could routinely be obtained by this method. The merit of the present method is its extreme simplicity by which one can deposit useful tin dioxide films for device applications either on one side or both sides of a planar substrate or inside of a tube quite easily in any laboratory.

References

[1] K.L. Chopra, S. Major, D.K. Pandya, Thin Solid Films 102 (1983) 1–46.
[2] C.S. Rastomjee, R.S. Dale, R.J. Schaffer, F.H. Jones, R.G. Egdell, G.C. Georgiadis, M.J. Lee, T.J. Tate, L.L. Cao, Thin Solid Films 279 (1996) 98–105.
[3] I. Kocemba, T. Paryjczak, Thin Solid Films 272 (1996) 15–17.
[4] B.J. Hwang, K.L. Lee, Thin Solid Films 279 (1996) 236–241.

[5] E. Shanthi, V. Dutta, A. Banerjee, K.L. Chopra, J. Appl. Phys. 51 (12) (1980) 6243–6251.
[6] E. Shanthi, A. Banerjee, K.L. Chopra, Thin Solid Films 88 (1982) 93.
[7] G. Gordillo, L.C. Moreno, W. de la Cruz, P. Teheran, Thin Solid Films 252 (1994) 61–66.
[8] A.L. Unaogu, C.E. Okeke, Solar Energy Mater. 20 (1990) 29–36.
[9] H. Kim, H.A. Laitimen, J. Am. Ceram. Soc. 58 (1975) 23.
[10] E. Shanthi, A. Banerjee, V. Dutta, K.L. Chopra, Appl. Phys. 53 (1982) 1615.
[11] G. Maurodien, M. Gajardziska, Novkovski, Thin Solid Films 113 (1984) 93.
[12] J. Bruneaux, H. Cachet, M. Froment, A. Messad, Thin Solid Films 198 (1991) 129–142.
[13] J. Proscia, R.G. Gordon, Thin Solid Films 214 (1992) 175–187.
[14] Yan Dawei, Ma Xiaocui, Wang Zongchang, Wu Jam, Thin Solid Films 224 (1993) 257–262.
[15] A. Fujisawa, T. Nishino, Y. Hamakawa, Jpn. J. Appl. Phys. 27 (4) (1988) 552–555.
[16] M.R. Kadam, N. Vittal, R.N. Karekar, R.C. Aiyar, Thin Solid Films 187 (1990) 199.
[17] B.J. Baliga, S.K. Ggandi, J. Electrochem. Soc. 123 (1976) 941.
[18] J.P. Chatelon, C. Terner, E. Bernstein, R. Berjoan, J.A. Roger, Thin Solid Films 247 (1994) 162–168.
[19] C.J. Brinker, A.J. Hurd, P.R. Schunk, G.C. Frye, C.S. Ashley, J. Non-Cryst. Solids 147&148 (1992) 424–436.
[20] Y. Takahashi, Y. Wada, J. Electrochem. Soc. 137 (1990) 267.
[21] H. Demiryont, N. Tezey, Thin Solid Films 101 (1983) 345.
[22] A. Czapla, E. Kusior, M. Bucko, Thin Solid Films 182 (1989) 15.
[23] M.K. Karanjai, D. Dasgupta, J. Phys. D 21 (1988) 356–358.
[24] H. Dislich, E. Hyssmann, Thin solid films 77 (1980) 129–142.
[25] J.L. Vossen, in: G. Hass, M.H. Francombe, R.W. Hoffmann (Eds.), Physics of Thin Films, Vol. 9, Academic Press, New York, 1977, pp. 1–71.
[26] A. De, S. Ray, J. Phys. D 24 (1991) 719–726.
[27] J.C. Manifacier, L. Szepessy, J.F. Bresse, M. Perotin, R. Stuck, Mater. Res. Bull. 14 (1979) 163.
[28] G. Haacke, J. Appl. Phys. 47 (9) (1976) 4086–4089.
[29] J. Kane, H.P. Schweizer, W. Kern, J. Electrochem. Soc. 122 (1975) 1144.
[30] J. Kane, H.P. Schweizer, W. Kern, J. Electrochem. Soc. 123 (1976) 270.

ELSEVIER

Surface and Coatings Technology 102 (1998) 73–80

SURFACE & COATINGS TECHNOLOGY

Tin dioxide based transparent semiconducting films deposited by the dip-coating technique

Sekhar C. Ray, Malay K. Karanjai, Dhruba DasGupta *

Department of Physics, University of North Bengal, Siliguri, Darjeeling-734430, West Bengal, India

Received 29 April 1997; accepted 22 September 1997

Abstract

Undoped and F-doped transparent semiconducting films with tin dioxide as the active material have been prepared by a dip-coating technique. The film is formed in situ by the hydrolysis of stannous chloride which takes place when a substrate is withdrawn vertically from a methanol solution of $SnCl_2 \cdot 2H_2O$ and heat treated at a high temperature. F-doping is achieved by adding NH_4F to the starting solution. The maximum film thickness obtainable per dipping cycle is about 0.58 μm, but can be increased by multiple dipping. The films appear to be a mixed phase consisting of crystalline tin oxide over an amorphous background probably of Sn(OH)Cl. The film produced by a single dipping consists of a small number of isolated SnO_2 crystallites. But as the film thickness is increased these crystallites increase in number and finally merge into a continuous layer. A typical value of resistivity for F-doped films produced by this method is 2.4×10^{-2} Ω cm, with an average transmission of >85% at a thickness of 2.96 μm. © 1998 Elsevier Science S.A.

Keywords: Transparent semiconducting oxide; SnO_2-based thin films; Dip-coating technique

1. Introduction

Among transparent conducting oxide materials, tin dioxide films find wide use because of their excellent performance along with high mechanical, chemical and environmental stability and low cost. In recent years extensive studies have been carried out on these films, which are characterized by high electrical conductivity and high transparency in the visible region of the solar spectrum combined with a high reflectivity in the infrared (IR) region. Tin dioxide is a semiconductor with a wide band gap (3.5–4 eV) [1–3] having a refractive index of approximately 2.0 [3] and a tetragonal crystal structure. The material is used in a variety of display devices such as liquid crystal displays, electrochromic and electroluminescent cells and imaging tubes [4–6] such as photovoltaic devices.

A variety of techniques have been employed to deposit tin dioxide films. These include reactive sputtering [7], spray pyrolysis [8,9], "paste–heat" [10], chemical vapour deposition [11,12] and reactive evaporation [13].

The dip-coating technique is an extremely simple and low-cost method for the deposition of oxide thin films [14]. In this method, as in the related sol gel method [15,16], a metal oxide film is produced by hydrolysis of the corresponding metal alkoxide, nitrate or chloride on a substrate and subsequently heat treated at a high temperature. There are however, few reports in the literature on SnO_2 films prepared by this method, which tend to have a resistivity of at least an order of magnitude higher than those prepared by other techniques, such as chemical vapour deposition (CVD) [17]. This high value of resistivity, while not suitable for photovoltaic cells, would not be a problem for low current applications, such as liquid crystal displays. The present work describes the preparation of undoped and F-doped tin dioxide-based transparent semiconducting thin films by the dip-coating technique and results of study of their electrical and optical properties as well as surface morphology and crystal structure.

2. Experimental details

To prepare the films, the substrate is first dipped and then withdrawn vertically from a solution of

* Corresponding author

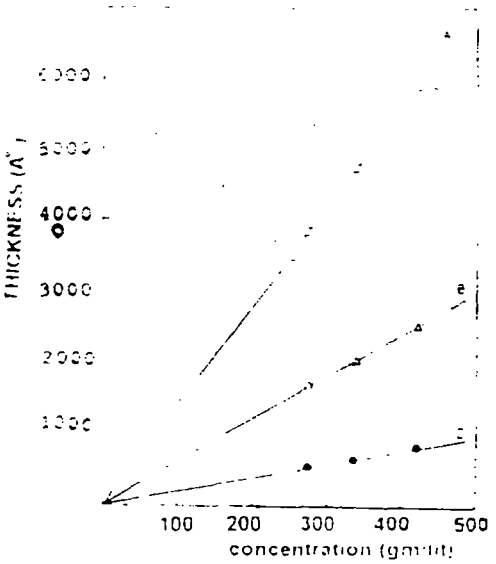

Fig. 1. Variation of thickness of films, deposited on glass substrates, with concentration of the starting solution [speed of withdrawal: A = 3 mm s, B = 1.3 mm s, C = 0.56 mm s].

$SnCl_2 \cdot 2H_2O$ in methanol at a controlled speed (1.33 mm s). The substrate together with its adhering liquid film is then transferred to a furnace kept at a high temperature and heat treated in air for 5 min. Details of the process are given elsewhere [18]. For doped film preparation, the requisite amount of ammonium fluoride is added to the starting solution.

Undoped and doped films were prepared for different heat-treatment temperatures. Variation of thickness with lifting speed and concentration was studied. Thicker films could be obtained by repeating the whole cycle (dip–withdrawal–heat treatment) a number of times.

Films were deposited on soda-glass microscope slides and mica sheets. The characterization was mostly done on those deposited on glass substrates.

The thickness of the deposited films was measured using the stylus method, while sheet resistance was measured by a standard four probe arrangement. Optical transmission as a function of wavelength was obtained by SHIMADZU UV-240 double-beam spectrophotometer. Surface morphology and X-ray diffractometric studies were carried out with a HITACHI S-530 scanning electron microscope and a PHILIPS diffractometer (model PW 1390) with CuK$_\alpha$ radiation.

3. Results

It was found that a heat-treatment temperature of 400–500 C was necessary to obtain films of useful quality in terms of low sheet resistance and high optical transmission. Within this temperature range there was no noticeable variation in the film properties. Results reported in this paper refer to films prepared at a heat-treatment temperature of 400 C.

4. Thickness

Figs. 1–3 show the variation of film thickness with speed of withdrawal, concentration and number of dippings, respectively. It is observed that the thickness

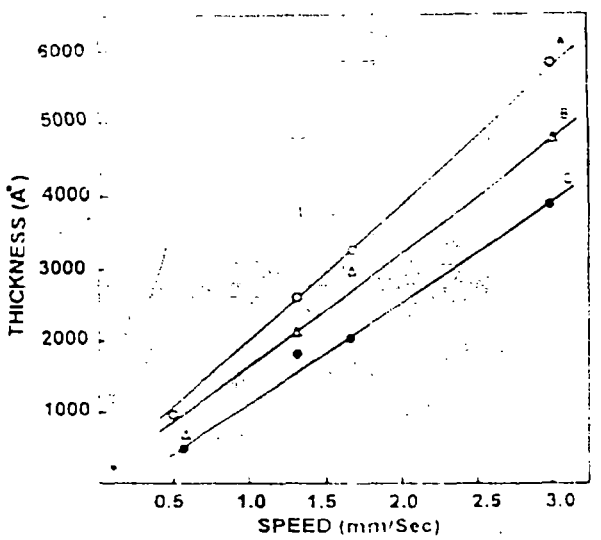

Fig. 2. Variation of thickness of films, deposited on glass substrates, with speed of withdrawal [concentration of the starting solution: A = 410 g l; B = 330 g l; C = 250 g l].

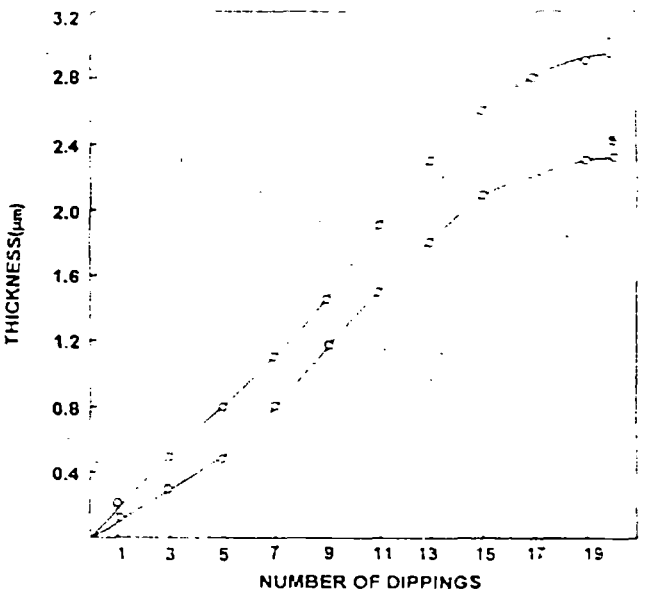

Fig. 3. Variation of thickness of films, deposited on glass substrates, with number of dippings at a speed of withdrawal 1.3 mm s [concentration of the starting solution: A = 330 g l, B = 250 g l].

of the deposited layer increases linearly up to 7–8 dippings, beyond which the rate of increase is slower.

5. X-ray diffractometric study

Fig. 4 shows the X-ray diffractograms of undoped films on glass substrate for five different numbers of dippings. It is evident from the diffractograms that crystallinity of the films increased with number of dippings up to a value of 20 dippings. Single dip films are predominantly amorphous.

Fig. 5 shows the X-ray diffractogram of a typical 10 dip film on mica substrate. The peaks are observed to be much sharper compared to those for films deposited on soda-glass substrates. The position of the peaks obtained on both glass and mica substrates are in conformity with the standard tetragonal crystal structure of SnO_2. Comparison with ASTM (I/I_0) data indicates that there is no significant preferential growth in any direction.

6. Electrical properties

Fig. 6 shows the decrease in sheet resistance of undoped and F-doped films (4.5 at.%) with thickness. The lowest values of sheet resistance, of undoped and 4.5 at.% F-doped films, are 300 Ω and 80 Ω, respectively, for a thickness of 2.96 μm which corresponds to resistivity values of 8.9×10^{-2} Ω cm and 2.4×10^{-2} Ω cm, respectively.

It was found that a film prepared by single dipping in a high concentration solution has a much higher value of sheet resistance compared to one having the same thickness but prepared by multiple dippings using a lower concentration dip solution. For example, at a thickness of 0.58 μm the sheet resistance of a single dip

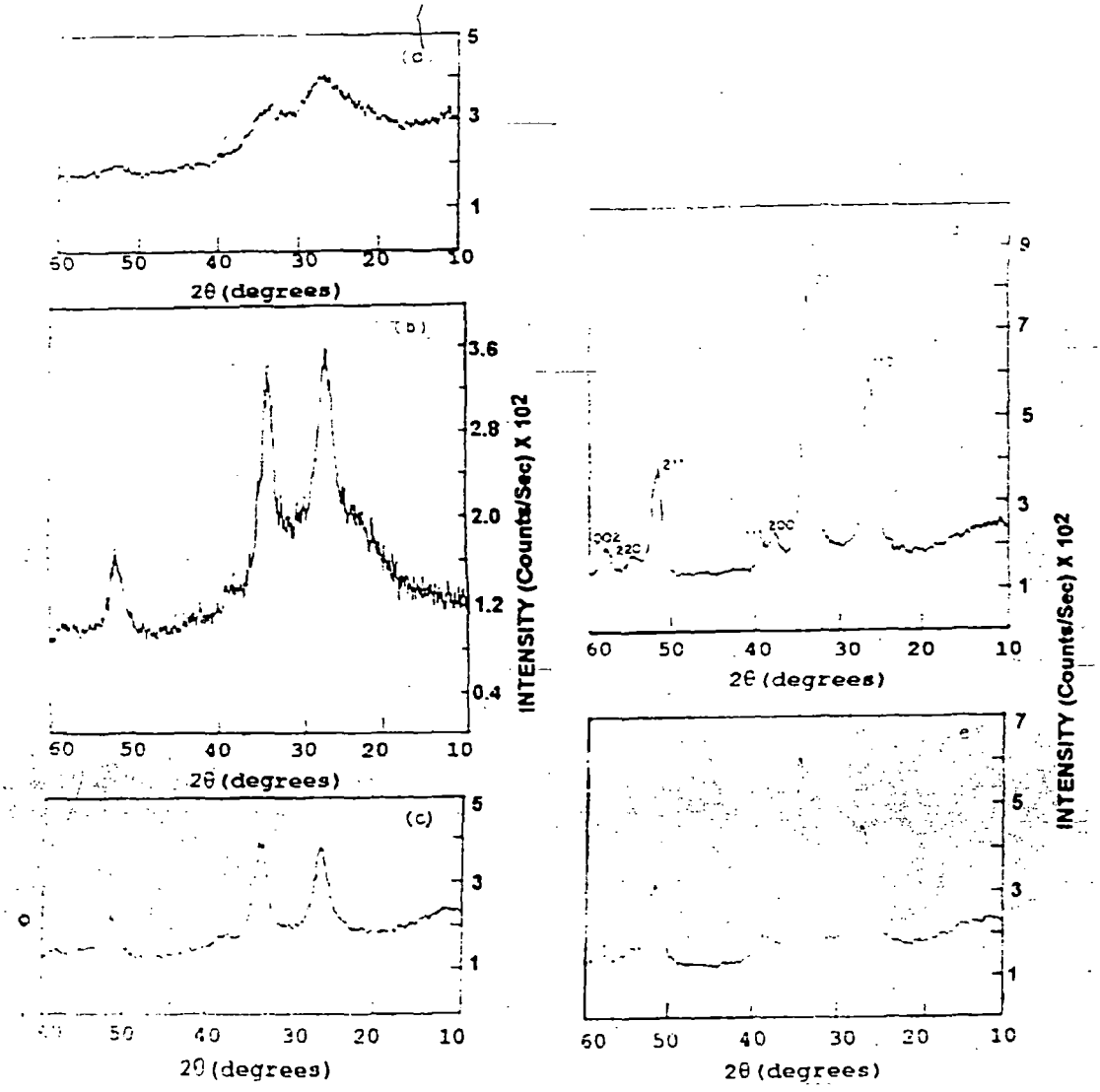

Fig. 4. X-ray diffractograms of dip coated undoped film on glass substrate: (a) 1st dip; (b) five dips; (c) ten dips; (d) twenty dips; (e) twenty five dips.

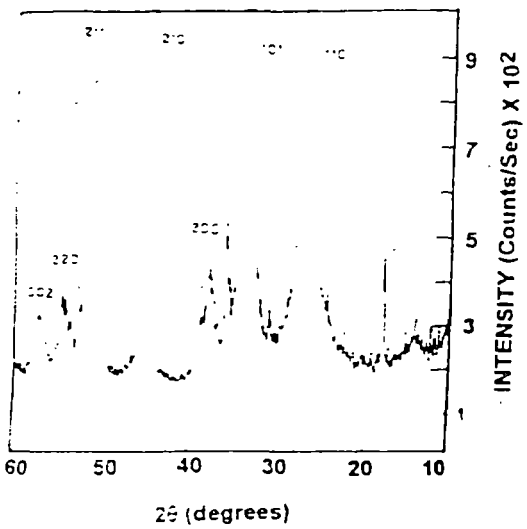

Fig. 5. X-ray diffractograms of a typical film on mica substrate (ten dips). Peaks which are unmarked do not correspond to SnO_2 and probably arise from the substrate itself.

film was $4 \cdot 10^4\ \Omega$, while that prepared by five dippings was $8 \cdot 10^3\ \Omega$. The possible reason may be that for single dipping, a number of loosely packed crystallites are formed, while for multi-dipping these crystallites formed at every deposition step tend to merge together and produce a continuous conducting path. Support for this argument is obtained from Fig. 6, where the sheet resistance of undoped films is seen to drop sharply at a thickness of about 1 μm. For F-doped films the drop occurs at a thickness of about 0.5 μm.

7. Surface morphology study by SEM

Fig. 7 shows the scanning electron micrographs of undoped and 4.5 at.% F-doped films. It is clear from the micrographs that for the undoped film, grain size increases up to 20 dippings. The initial layer (1st dip) films over an amorphous glass substrate is nearly amorphous which is evidenced from the XRD pattern also. Fig. 8 shows the surface morphologies of the films on mica. The grain size is considerably larger in the case of mica substrate than that on glass substrate (Fig. 7e). The much sharper XRD peaks observed in this case are also consistent with the larger grain size. It is possible that formation of bigger crystallites is facilitated by the single-crystal substrate, which is in contact with the growing film.

8. Optical properties

Films obtained by dip-coating technique are highly transparent. Fig. 9 shows the optical transmission *versus* wavelength curves for undoped and 4.5 at.% F-doped films with different sheet resistance values. It is seen that the optical transmission is reduced as a result of doping.

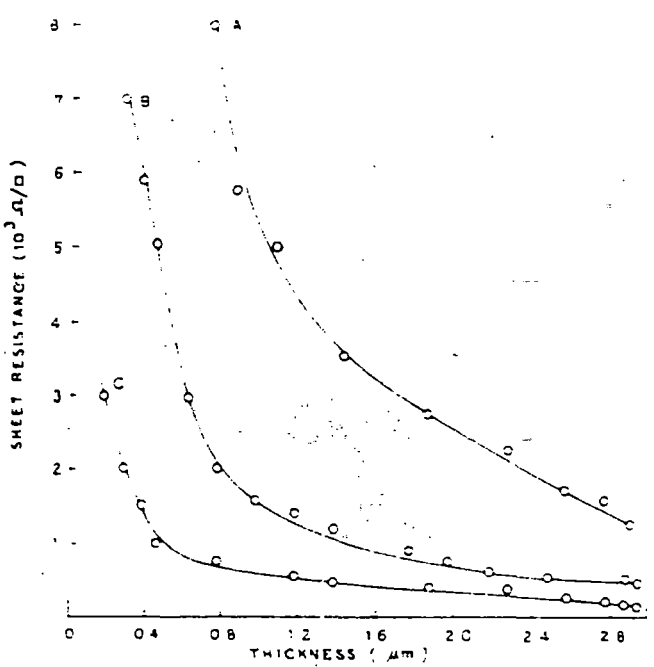

Fig. 6. Variation of sheet resistance of film deposited on glass substrates with thickness. Undoped: A = 250 g l; B = 330 g l. 4.5 at.% F-doped: C = 250 g l.

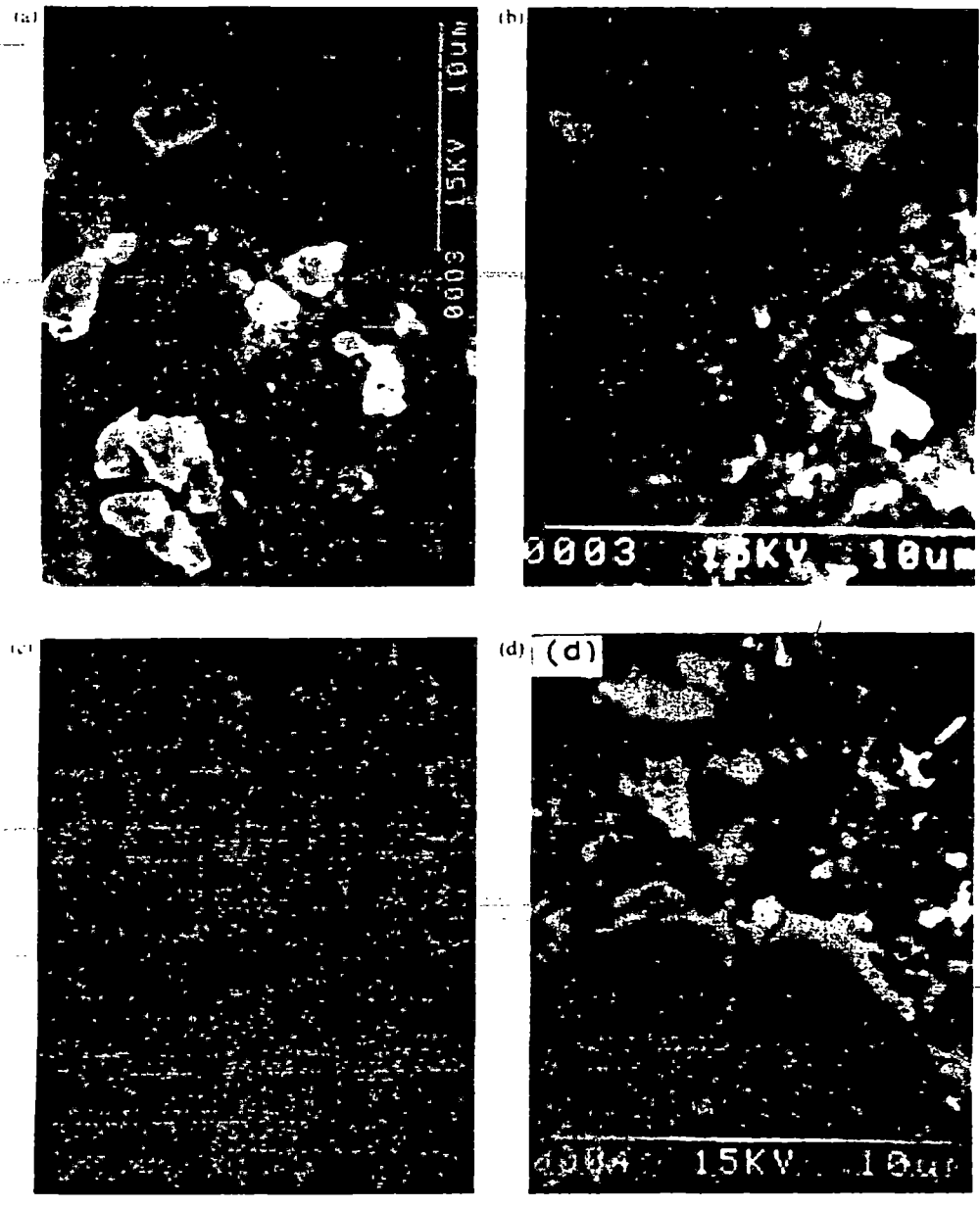

Fig. 7. Electron micrographs of undoped and doped films on glass substrate. Undoped: (a) 1st dip; (b) five dips; (c) ten dips; (d) fifteen dips; (e) twenty dips; (f) twenty five dips. 4.5 at.% F-doped film: (g) twenty dips.

A similar phenomenon has also been observed by Chopra et al. [4] and De et al. [19] and attributed by them to a high surface roughness of SnO_2 films having low sheet resistance compared to undoped ones. Average optical transmission 85–90% for undoped and 75–80% for F-doped films are obtained for a thickness of 2.96 μm over a range 400 to 900 nm.

9. Discussion

It is known [10,20] that $SnCl_2$ undergoes hydrolysis according to the equation

$$6SnCl_2 + H_2O \rightarrow 2SnCl_4 + 4Sn(OH)Cl \quad (1)$$

This reaction is relatively slow at room temperature, but is accelerated on heating. $SnCl_4$, in turn, readily hydrolyses to SnO_2 at a high temperature as given below

$$SnCl_4 + 2H_2O = SnO_2 + 4HCl \quad (2)$$

This forms the basis of preparation of conducting tin dioxide films by the paste–heat or OACVD methods [10,21]. In these methods, $SnCl_4$ produced from reaction (Eq. (1)) taking place in a separate area is allowed to hydrolyse on the substrate and yield SnO_2. In contrast, in the present method the Sn(OH)Cl also remains on the substrate and forms the amorphous matrix, while most of the $SnCl_4$ produced, escapes. A small fraction of this $SnCl_4$, however, is hydrolysed on the substrate

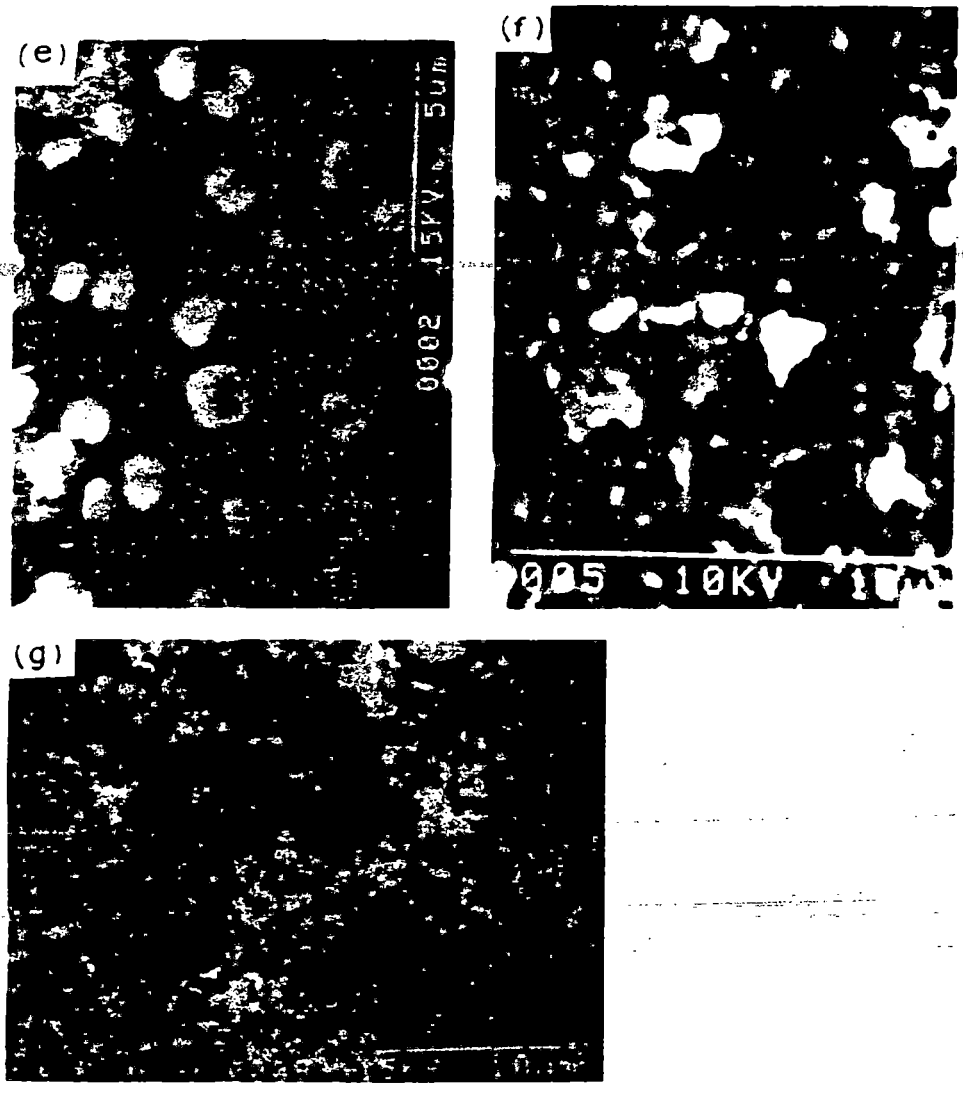

Fig. 7. (*continued*)

and produces small SnO_2 crystallites. Repeated dipping increases the number of these crystallites which form an interconnected network after about 15–20 dippings. This can be seen from the XRD spectra, the variation of sheet resistance with thickness and the SEM photographs. We see that the sharp drop in sheet resistance, appearance of sharp XRD peaks and merging of SnO_2 grains, all take place at a thickness of about 1 μm. However, even at this stage the proportion of the amorphous component is quite large, as shown by the high value of resistivity, viz. $2.4 \times 10^{-2}\,\Omega$ cm compared to $2.4 \times 10^{-4}\,\Omega$ cm for CVD SnO_2 films. It may be interesting to note that in the work of Gordillo et al. [22], also on spray-deposited SnO_2 films, a strong amorphous background is seen to be present in the XRD pattern when $SnCl_2$ was used as a starting material.

Although this amorphous component, most probably Sn(OH)Cl, is present in the films, it is highly transparent and leads to no significant drop in optical transmission. This component is responsible for making the resistivity about two orders of magnitude higher than that obtained for CVD films. However, the high optical transmittance makes these films suitable for those display applications where the current requirement is low, e.g. liquid crystal or electrochromic displays. In addition, the simplicity of the deposition method could make it attractive for enhancing the IR reflectivity at a low cost, e.g. in solar cookers.

The effectiveness of a transparent conducting film depends on its optical transmission as well as its sheet resistance. As already discussed, the high sheet resistance of the dip-coated films is, to a great extent, compensated for by their large optical transmittance. Haacke [23] has introduced a figure of merit for transparent conducting films defined by the relation $\varphi_{TC} = T^{10} R_S$, where T is the optical transmittance and R_S is the sheet resistance. This parameter can be used to evaluate the performance of a candidate material from its fundamental parame-

Fig. 8. Electron micrograph of undoped film on mica substrates (10 dips).

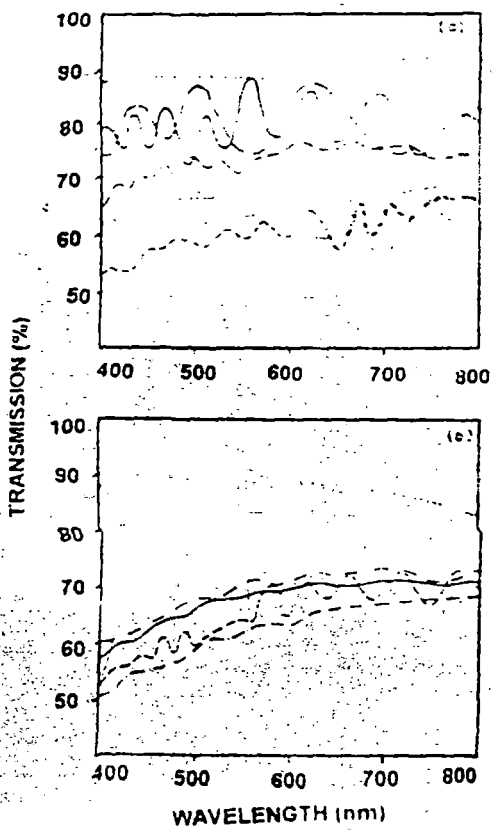

Fig. 9. Optical transmission *versus* wavelength for typical films of various sheet resistances. (a) Undoped: (.....), bare substrate; (——), 4000 Ω; (-.-.-.), 1250 Ω; (- - - -), 600 Ω; (), 250 Ω; (b) 4.5 at.% F-doped films: (.....), bare substrate; (——), 800 Ω; (), 500 Ω; (- - - -), 200 Ω; (-.-.-.), 90 Ω.

ters. A typical σ_{fc} value for our 4.5 at.% F-doped, dip-coated film is $2.5 \times 10^{-3}\ \Omega^{-1}$, which compares quite favourably with the value of $2.6 \times 10^{-3}\ \Omega^{-1}$ for CVD SnO_2 films [24,25].

10. Summary

It has been demonstrated that the dip-coating technique can be used to deposit transparent semiconducting films in a simple manner using $SnCl_2 \cdot 2H_2O$ as a starting material. The films contain crystalline SnO_2 in addition to an amorphous background, probably of Sn(OH)Cl. The resistivity of the films is somewhat higher compared to SnO_2 films prepared by CVD or spray pyrolysis. This is probably due to the presence of the amorphous constituent. However, the films are highly transparent and have a figure of merit comparable to that for conventionally-prepared SnO_2 films. The films would be potentially useful for low-current application such as display devices. The method is easily adaptable for deposition on large-area surfaces.

References

[1] J.C. Manifacier, L.D. Zepessy, J.F. Bresse, M. Perotin, Mater. Res. Bull. 14 (1979) 163.
[2] W. Spence, J. Appl. Phys. 38 (1967) 3767.
[3] Y.S. Hsu, S.K. Gandhi, J. Electrochem. Soc. II: Sol. State Sci. Technol. 127 (1980) 1592.
[4] K.L. Chopra, S. Major, D.K. Pandya, Thin Solid Films 102 (1983) 1.
[5] C.S. Rastomjee, R.S. Dale, R.J. Schaffer, P.H. Jones, R.G. Lodell, G.C. Georoiadis, M.J. Lee, T.J. Tate, L.L. Cao, Thin Solid Films 279 (1996) 98.
[6] J. Kocemba, T. Paryjczak, Thin Solid Films 272 (1996) 15.
[7] T. Matsuoka, J. Kuwata, M. Nishikawa, V. Fujita, T. Tohda, A. Abe, Jpn J. Appl. Phys. 27 (1988) 1088.
[8] E. Shanthi, V. Dutta, A. Banerjee, K.L. Chopra, J. Appl. Phys. 51 (1980) 6243.
[9] B.J. Baliga, S.K. Gandhi, J. Electrochem. Soc. 123 (1976) 941.
[10] M.K. Karanjai, D. DasGupta, J. Phys. D: Appl. Phys. 21 (1988) 356.
[11] T.P. Chow, M. Ehezzo, B.J. Baliga, J. Electrochem. Soc. 129 (1982) 1040.
[12] J.P. Upadhayay, S.R. Vishwakarma, H.C. Prasad, Thin Solid Films 169 (1989) 195.
[13] H. Demryont, N. Tezzy, Thin Solid Films 101 (1983) 345.
[14] H. Dislich, E. Hussmann, Thin Solid Films 77 (1981) 129.
[15] J.P. Chatelon, C. Terrier, E. Bernstein, R. Berjoan, J.A. Roger, Thin Solid Films 247 (1994) 162.
[16] C. Terrier, J.P. Chatelon, R. Berjoan, J.A. Roger, Thin Solid Films 263 (1995) 37.
[17] S. Sakka, J. Non-crystalline Sol. 73 (1985) 651.
[18] M.K. Karanjai, D. DasGupta, Thin Solid Films 155 (1987) 309.
[19] A. De, S. Ray, J. Phys. D: Appl. Phys. 24 (1991) 719.

[20] J.R. Partington, A Text Book of Inorganic Chemistry 6th edn. MacMillan, London, 1950, p. 829.
[21] S.C. Ray, M.K. Karanjai, D. DasGupta, Thin Solid Films 307 (1997) 221.
[22] G. Gordillo, L.C. Moreno, W. De la Cruz, P. Teheran, Thin Solid Films 252 (1994) 66.
[23] G. Hacke, J. Appl. Phys. [illegible] (1976) 4056.
[24] J. Kane, H.P. Schweizer, W. Kern, J. Electrochem. Soc. [illegible] (1975) 1144.
[25] J. Kane, H.P. Schweizer, W. Kern, J. Electrochem. Soc. [illegible] (1976) 270.

Reprints

ELSEVIER

Thin Solid Films 10619 (1998) xxx C

Thin Solid Films

Deposition and characterization of $Zn_xCd_{1-x}S$ thin films prepared by the dip technique

Sekhar C. Ray, Malay K. Karanjai, Dhruba DasGupta *

Department of Physics, University of North Bengal, Siliguri, Darjeeling-734430, West Bengal, India

Received 30 May 1997; accepted 16 October 1997

Abstract

$Zn_xCd_{1-x}S$ ($0 \le x \le 1$) thin films have been deposited by the dip technique on glass substrates. In this method, a clean substrate was dipped into an alcoholic solution of the corresponding nitrates and thiourea and then withdrawn vertically at a controlled speed, and finally baked in a furnace. X-ray diffractometric study suggests that for zinc atomic fraction $x \le 0.6$ films prepared at a baking temperature of 500°C are homogeneous with a hexagonal (wurtzite) structure. Increase in the proportion of zinc in the starting solution is found to produce a decrease in the lattice parameter. SEM studies reveal an increase in grain size with x up to a value of 0.6. For $x > 0.6$, the films appear to have an amorphous character, as no distinguishable peaks can be seen in the X-ray diffractograms. The SEM micrographs also do not show any clearly defined grains over this range. Values of bandgap obtained from optical absorption measurements as well as from spectral response of photoconductivity are in good agreement with each other and vary monotonically from 2.30 eV (CdS) to 2.69 eV ($Zn_{0.6}Cd_{0.4}S$) over the range $0 \le x \le 0.6$. © 1998 Elsevier Science S.A.

Keywords. Deposition process; Optical properties; Surface morphology; X-ray diffraction

1. Introduction

$Zn_xCd_{1-x}S$ thin films have been widely used as wide bandgap window material in heterojunction photovoltaic solar cells [1–5] and in photoconductive devices [6]. In solar cell systems, where CdS thin films have been proved to be useful, partial substitution of Zn for Cd increases the optical window of the heterojunction and also the diffusion potential [7]. Moreover, in heterojunction solar cells using $CuGaSe_2$, the use of $Zn_xCd_{1-x}S$ instead of CdS can lead to an increase in photocurrent by providing a match in the electron affinities of the two materials. This hexagonal $Zn_xCd_{1-x}S$ ternary compound is also potentially useful as a window material for the fabrication of *p–n* junctions without lattice mismatch in the devices based on quaternary materials like $CuIn_xGa_{1-x}Se_2$ [8] or $CuIn(S_zSe_{1-z})_2$ [9]. $Zn_xCd_{1-x}S$ thin films have been prepared by a variety of techniques, which include spray pyrolysis [7,10], ion beam deposition [11], molecular beam epitaxial growth [12], solution growth [13,14], and successive ionic layer absorption and reaction process [15].

The dip technique and the related sol–gel method have been traditionally used for the deposition of oxide thin films [16,17]. Usually, these involve the hydrolysis of the corresponding metal alkoxide, nitrate or chloride on a heated substrate. In a previous work [18], we reported a modification of the dip technique for the deposition of sulphide films. Here, the substrate is withdrawn from an alcoholic solution of the metal nitrate and thiourea, and transferred to a furnace maintained at a high temperature, where a chemical reaction takes place to yield the sulphide films.

As described in Ref. [18], attempts to produce $Cd_{0.8}Zn_{0.2}S$ films using a starting solution containing both cadmium and zinc nitrates resulted in the formation of a mixed phase material containing partially crystalline CdS and amorphous ZnS when prepared at a baking temperature of 400°C. It has been found that by increasing the baking temperature to 500°C homogeneous crystalline $Zn_xCd_{1-x}S$ films within the range $0 \le x \le 0.6$ could be produced. These shows continuous variation of lattice parameter and bandgap as a function of x. For $x > 0.6$, the films tend to develop an amorphous character. The bandgap varies monotonically from 2.3 eV (CdS) to 2.69 eV ($Zn_{0.6}Cd_{0.4}S$) over the range $0 \le x \le 0.6$. We describe in

* Corresponding author. Tel.: +91-353-450414; fax: +91-353-450546; e-mail: dhruba@nbu.ernet.in

PII S0040-6090(97)00932-2

this report the preparation of these films and their characterization by X-ray diffractometry, scanning electron microscopy, optical and photoconductivity measurements.

2. Experimental details

Three separate saturated solutions of cadmium nitrate [$Cd(NO_3)_2$, $4H_2O$], zinc nitrate [$Zn(NO_3)_2$, $6H_2O$] and thiourea with methanol as solvent were initially prepared. They were then mixed in requisite amounts to yield the starting solution for deposition by dipping. It was found that the mixing was best achieved without any precipitation taking place if the thiourea solution was divided into two parts which were mixed with the two nitrate solutions separately, and one of the mixtures then slowly added to the other.

Microscope glass slides, used as substrates, were cleaned by washing in detergent and chromic acid and finally degreased in acetone and methanol vapour.

In the film forming process, a clean substrate was dipped into the starting solution and then withdrawn vertically at a controlled speed, under atmospheric conditions, with the help of a pulley and geared motor, when a liquid film adhered to the substrate. The substrate together with the liquid film adhering to it was immediately transferred to a furnace for baking, when the chemicals reacted to form the desired solid film. It is found that films of a very high quality were obtainable when prepared at a baking temperature of 500°C. Thickness of the films could be increased by repeating the whole cycle (dip–withdrawal–bake) a number of times. Details are given in Ref. [18].

$Zn_xCd_{1-x}S$ films were deposited at 500°C for various concentrations of zinc from $x = 0$ to $x = 1$. The value of x was changed by changing the concentrations of Zn–nitrate and Cd–nitrate in the starting solution. The Zn/Cd ratio in the solid films was determined by Atomic Absorption Spectroscopy. The value of x was found to be essentially the same as the relative proportion of Zn atoms [Zn:(Zn + Cd)] in the starting solution. Film thickness was measured by stylus method. Characterization of the films was carried out by optical absorption, X-ray diffractometry, scanning electron microscopy and spectral response of photo conductivity measurements.

Optical properties were studied by Shimadzu UV-240 double-beam spectrophotometer. X-ray diffractometry and surface morphology studies were carried out by Philips diffractometer (model PW 1390) with CuK_α radiation (Ni-filter) at 1.54 Å and Hitachi S-530 scanning electron microscope, respectively. To determine the photo conductive (PC) spectral response, a PC cell was fabricated by depositing Ag-electrodes in the usual interdigitated pattern, which was subsequently placed at the detector position of a Spectromom 202 spectrophotometer, and the photo current measured as a function of wavelength. The area of the cell was about 1 cm^2.

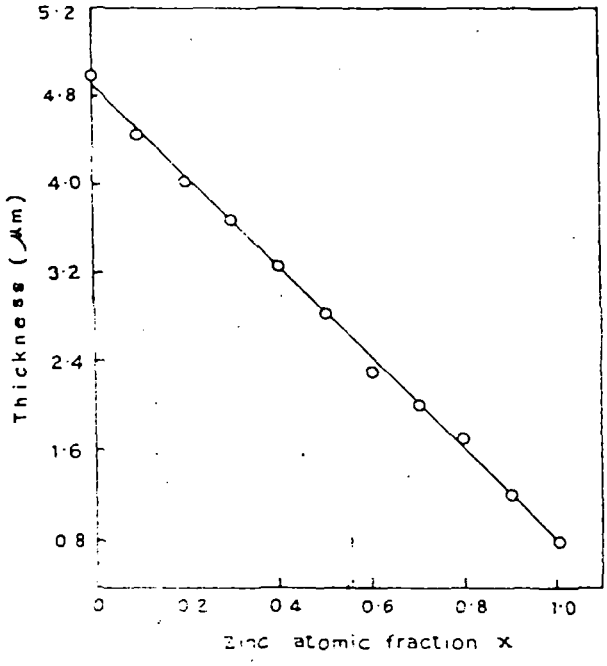

Fig. 1. Variation of thickness on zinc atomic fraction x of $Zn_xCd_{1-x}S$ thin films

3. Results and discussion

The $Zn_xCd_{1-x}S$ thin films were smooth, uniform, highly reflecting and strongly adherent to the substrate. Colour of the films was observed to change from yellow-orange to pale yellow with increase in zinc atomic fraction x. Zinc sulphide films ($x = 1$) were white in colour.

Films of different thicknesses were obtained by changing the lifting speed as well as increasing the number of dippings (dip–withdrawal–bake cycle). Smooth and uniform films could be obtained up to a maximum withdrawal speed of 1.33 mm/s. For higher speeds, the films tended to be non-uniform. At high withdrawal speeds, the liquid layer adhering to the substrate as it is pulled out is quite thick, and turbulence in this layer is also higher.

Results reported in this paper were obtained by measurements on films prepared by 10 dippings from a starting solution containing total 0.93 (Cd + Zn) mol/l and withdrawn at a speed of 1.33 mm/s.

3.1. Thickness

Fig. 1 shows the variation of the thickness of the film for different values of x, when the total number of (Cd + Zn) moles was kept constant in a given volume of the starting solution. Cd and Zn ratio in the solid films measured by Atomic Absorption Spectroscopy, agrees well with that in the starting solution for different concentrations. The thickness of the films is found to decrease linearly with the increase in zinc proportion.

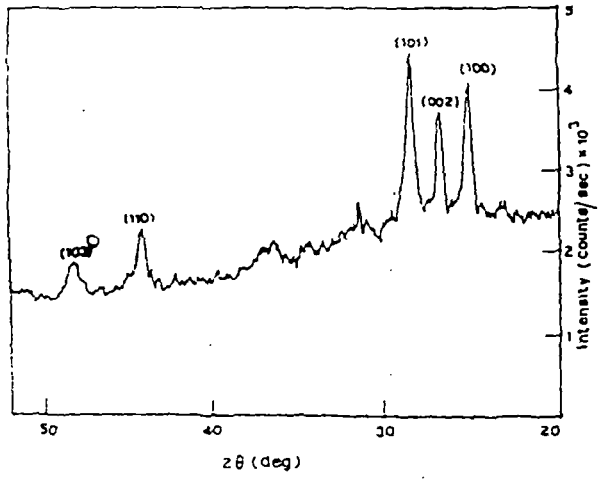

Fig. 2. X-ray diffractogram of a typical $Zn_xCd_{1-x}S$ thin film ($x = 0.4$).

3.2. X-ray diffractometric study

A typical XRD pattern for $Zn_xCd_{1-x}S$ (for $x = 0.4$) films is shown in Fig. 2. Comparison of the prominent peak positions (2θ-values) of the XRD spectra with the JCPDS data file for CdS [19] suggests that the $Zn_xCd_{1-x}S$ film deposited at a baking temperature of 500°C is hexagonal (wurtzite) in structure with the prominent X-ray diffraction peaks corresponding to (100), (002), (101), (110) and (103) planes.

It was observed that the diffraction angle (2θ) shifts to higher angles with increasing zinc atomic fraction x. The peaks, which are quite sharp up to $x = 0.4$, become weaker beyond this and no prominent peaks appear for $x > 0.6$, which means that in this range the films are mostly amorphous.

Fig. 3 shows the relationship between the lattice parameter and the zinc atomic fraction x over the range $0 \le x \le 0.6$. It is observed that the lattice constants decrease with increase in the proportion of Zn. This is consistent with the smaller size of the Zn atoms and also reflected in the decrease in thickness of the films with increasing x as described in Section 3.1. Similar results were obtained by Yamaguchi et. al [20]. The values of a and c for thin film prepared at $x = 0$ (pure CdS) are 4.13 Å and 6.73 Å, respectively. These values are in good agreement with the data for hexagonal CdS films from the JCPDS card [19].

3.3. Optical properties

The optical energy gap of the $Zn_xCd_{1-x}S$ thin film was estimated by measuring optical density (O.D.) of the films as a function of wavelength in the range 2.2 eV to 3.5 eV, from which absorption co-efficient (α) was obtained. Plots of $(\alpha h\nu)^2$ and $(\alpha h\nu)^{1/2}$ against $h\nu$ were made (Fig. 4). $(\alpha h\nu)^2$ vs. $h\nu$ plots yielded straight line over the range $0 \le x \le 0.6$. In contrast, for $x > 0.6$ straight lines were obtained when $(\alpha h\nu)^{1/2}$ was plotted against $h\nu$. This is indicative of the fact that the film are crystalline for $0 \le x \le 0.6$ and amorphous beyond this range.

Spectral response of photoconductivity curves are shown

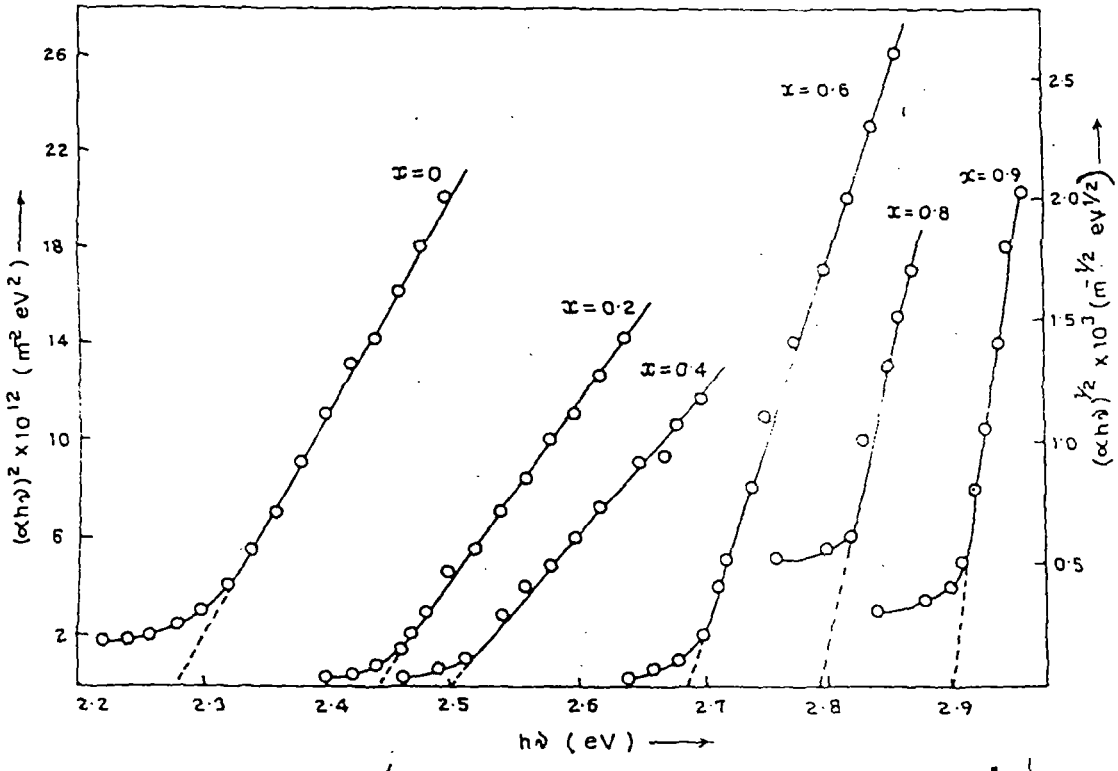

Fig. 4. The plots of $(\alpha h\nu)^2$ [for $0 \le x \le 0.6$] and $(\alpha h\nu)^{1/2}$ [for $x > 0.6$] against $h\nu$ of $Zn_xC_{1-x}S$ thin films

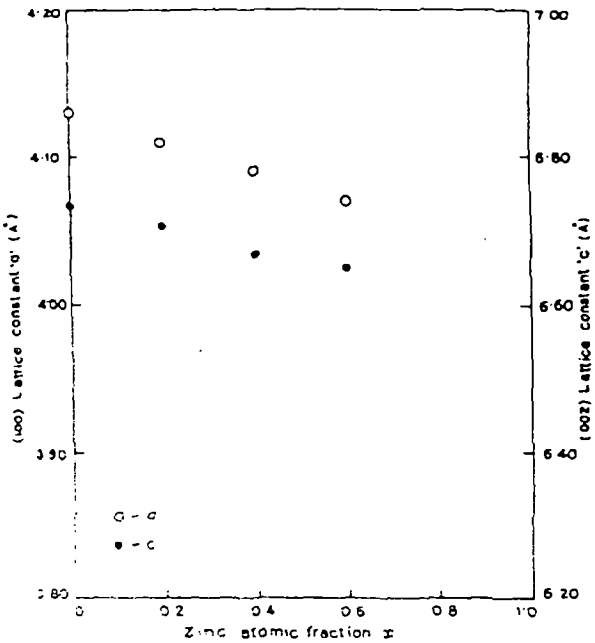

Fig. 3. The dependence of the lattice constants c and a on zinc atomic fraction x.

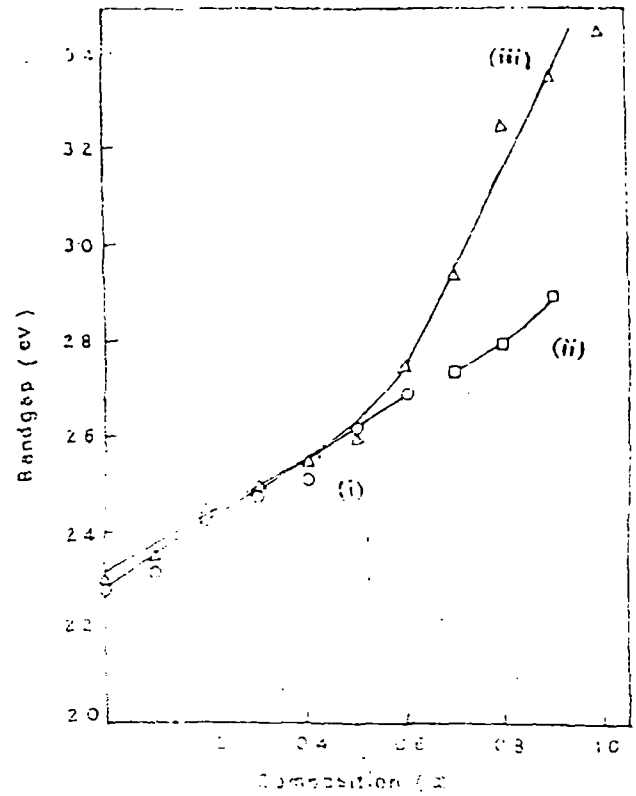

Fig. 6. Variation of (i) bandgap (○ ○ ○ ...) for $0 \le x \le 0.6$, (ii) optical bandgap (□ □ □ ...) for $x > 0.6$, and (iii) photon energy (Δ Δ Δ ...) with zinc atomic fraction x of $Zn_xCd_{1-x}S$ thin films.

in Fig. 5. The photocurrent values are normalized with the peak response for pure CdS taken as 1. No correction was made for the variation of intensity with wavelength of the tungsten filament source used in the spectrophotometer. With increasing x, position of the maximum moves from 540 nm for CdS to 360 nm for ZnS, corresponding to a shift in band gap from 2.3 eV to 3.4 eV. This continuous change in band gap with increasing proportion of zinc again confirms the formation of a solid solution.

Fig. 6 shows the variation with x of (i) bandgap for $0 \le x \le 0.6$, (ii) optical gap for $x > 0.6$, and (iii) the photon energy ($0 \le x \le 1$) at which peak response in photoconductivity is obtained. Curves (i) and (iii) agree quite closely in the range $0 \le x \lesssim 0.6$, where crystalline films

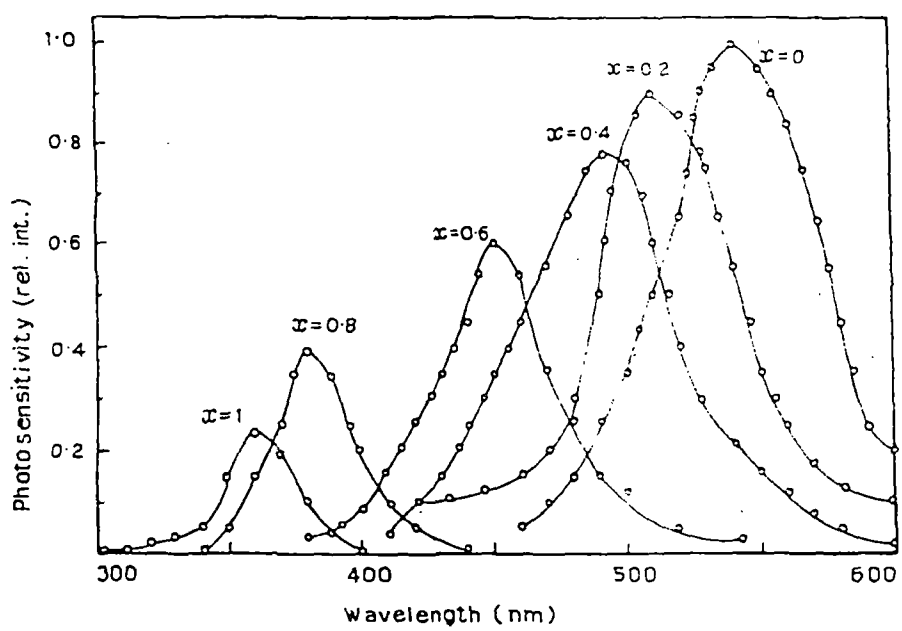

Fig. 5. The spectral response of photoconductivity curves of $Zn_xCd_{1-x}S$ thin films.

Ψ for peak photoconductive re

were obtained. The optical bandgaps for $x > 0.6$ are much less than that obtained from photoconductive measurements, which may be due to the amorphous nature of the films in that region.

According to H. Hill [21], the optical bandgap E_x of the $Zn_xCd_{1-x}S$ films can be expressed as:

$$E_{(x)} = E_{CdS} + (E_{ZnS} - E_{CdS} - b)x + bx^2$$

where b is the bowing parameter and x is Zn atomic fraction. The value of b for films is about 0.22 eV, estimated from curve fitting, with the values of optical bandgap in the range $0 \le x \le 0.6$. This value is in very close agreement with theory as obtained by Hill [21]. For $x > 0.6$, the value of b changes sharply to 0.07, again indicating a transition from crystalline to amorphous films.

3.4. Surface morphology

Fig. 7 shows the SEM micrographs of $Zn_xCd_{1-x}S$ th films for different values of zinc atomic fraction x. It evident from the micrographs that the grain size of the fil increases up to $x = 0.4$, beyond which a tendency reduction in crystallinity is observed. This is also ev denced in the XRD pattern, where sharp peaks are o served only over the range $0 \le x \le 0.4$.

4. Conclusion

Homogeneous and crystalline $Zn_xCd_{1-x}S$ thin film have been prepared successfully by the dip technique ov

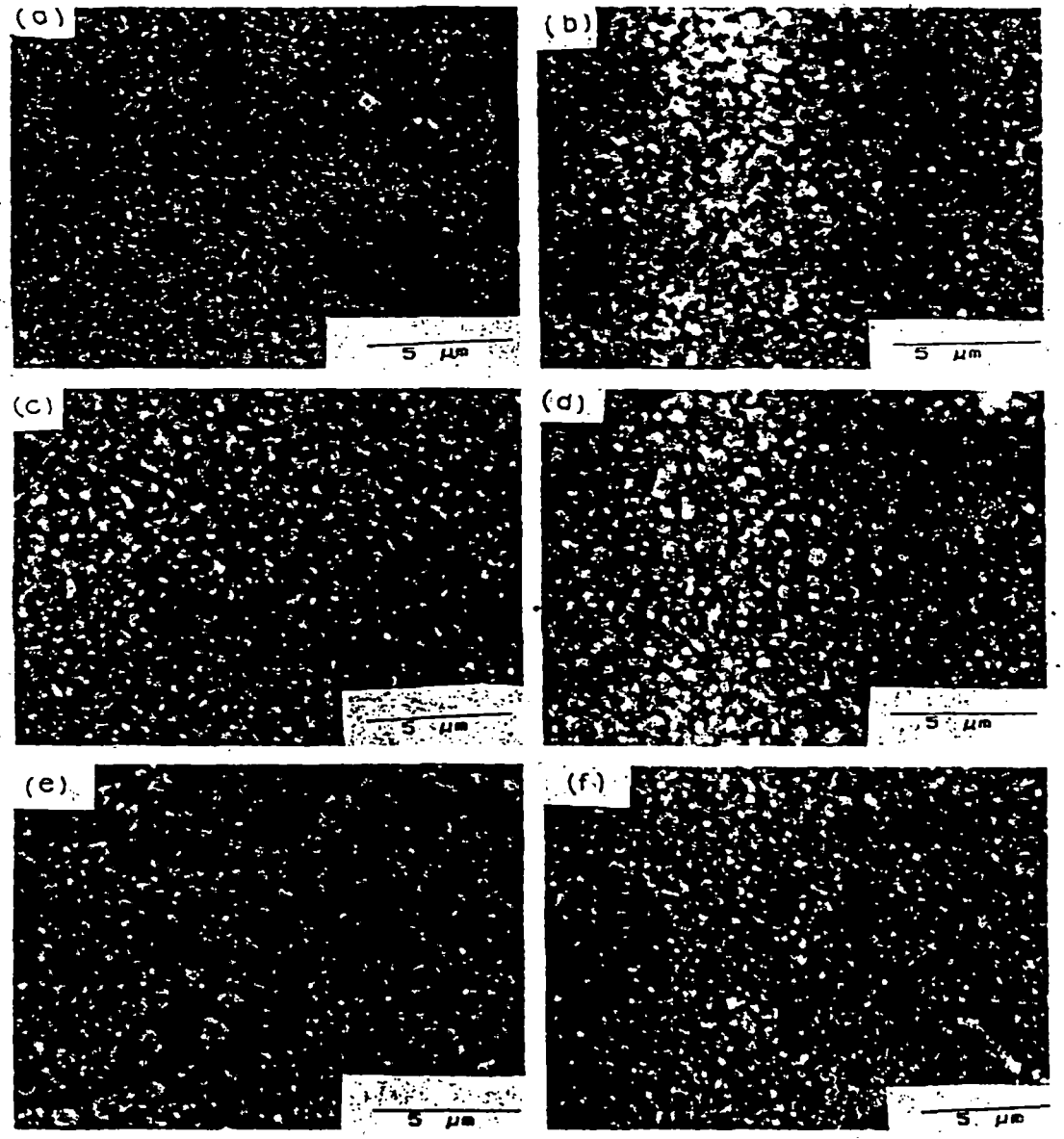

Fig. 7. The scanning electron micrographs of $Zn_xCd_{1-x}S$ thin films. (a) $x = 0$, (b) $x = 0.1$, (c) $x = 0.3$, (d) $x = 0.4$, (e) $x = 0.5$, (f) $x = 0.6$.

the range $0 \leq x \leq 0.6$ e films are hexagonal in structure, whose lattice parameters c and a are found to decrease with increase in x. An increase in x also produces a similar drop in the thickness of the film, when the total number of (Cd + Zn) moles in the starting solution is kept constant. This agrees well with the fact that the Zn atoms have a relatively smaller size compared to Cd atoms. The band gaps obtained from optical absorption and spectral response of photoconductivity measurements are in good agreement with each other and vary from 2.30 eV (CdS) to 2.69 eV ($Zn_{0.6}Cd_{0.4}S$), beyond which the bandgaps obtained from optical absorption measurements (optical gap) are much less than that obtained from photoconductive measurements. Surface morphology study by SEM as well as XRD data shows that good crystallinity is obtained up to a zinc atomic fraction of 0.4. For $x > 0.6$ the films appear to develop an amorphous character.

References

[1] K.T.R. Reddy, P.J. Reddy, J. Phys. D: 25 (1992) 1345.
[2] K.W. Mitchell, A.L. Fahrenbruch, R.H. Bube, J. Appl. Phys. 48 (1977) 4365.
[3] B.M. Basol, J. Appl. Phys. 55 (1984) 601.
[4] Y.K Jun, H.B Im, J Electrochem Soc.: Electrochem. Sci Techn 135 (1988) 1688
[5] H.S Kim, H.B Im, Thin Solid Films 214 (1992) 207
[6] J Torres, G Gordillo, Thin Solid Films 207 (1992) 231.
[7] T.A Chynoweth, R H Bube, J. Appl. Phys. 51 (1980) 1844
[8] T. Yamaguchi, J Matsufusa, A. Yoshida, Jpn J. Appl. Phys. (1992) L703
[9] T. Walter, M Ruckh, K O Velthaus, H.W. Schock, 1992, Proc. 11 EC Photovoltaic Solar Energy Conf., Montreux, p 124.
[10] A. Mzerd, D. Sayah, I.J. Saunders, B.K. Jones, Phys. Stat. Sol. 119 (1990) 487
[11] A. Kuroyanagi, Thin Solid Films 249 (1994) 91.
[12] T. Karasawa, K Ohkawa, T. Mitsuya, J. Appl. Phys. 69 (199 3226.
[13] Y.F. Nicolau, J.C. Menard, J. Cryst. Growth 92 (1988) 128.
[14] G.K. Padam, G L Malhotra, S.U M. Rao, J. Appl. Phys. 63 (198 770.
[15] Y.F Nicolau, M Dupuy, Electrochem. Soc 137 (1990) 2915.
[16] H. Schroeder, Oxide layers deposited from ...ic solutions, in: Hass, F Thun (Eds.), Physics of Thin Films, Vol. 5, Acaden Press, New York, pp 87–141, 1969.
[17] C. Terrier, J P. Chatelon, R. Berjoan, J.A. Roger, Thin Solid Fil 263 (1995) 37
[18] M.K. Karanjai, D Dasgupta, Thin Solid Films 155 (1987) 309.
[19] JCPDS, Swarthmore, PA, card no. 06-0314.
[20] T. Yamaguchi, Y Yamamoto, T. Tanaka, Y. Demizu, A. Yoshi Thin Solid Films 281–282 (1996) 375.
[21] H. Hill, J Phys C 7 (1974) 521.

140

PREPARATION AND STUDY OF MoS_2 THIN FILMS DEPOSITED B Y THE DIP TECHNIQUE

S.C.RAY, DEPARTMENT OF PHYSICS, UNIVERSITY OF NORTH BENGAL, SILIGURI DARJEELING - 734430, WEST BENGAL, INDIA AND
M.K.KARANJAI, DEPARTMENT OF PHYSICS, SILIGURI COLLEGE, SILIGURI, DARJEELING - 734401, WEST BENGAL, INDIA

Molybdenum sulphide (MoS_2) dichalcogenide thin film is a very promising semiconductor (bandgap 1.78 eV) for its various applications in solar cells, rechargeable batteries and as a solid lubricant for metallic and ceramic surfaces where hydrocarbon or other fluid-based lubricants are unsuitable, such as in high vacuum or high temperature applications MoS_2 thin films have been prepared by the dip technique In this technique, a clean glass substrate was dipped into the methanolic solution of ammonium molybdate and ammounium thiocyanate for half a min and then withdrawn vertically at a controlled speed, under atmospheric conditions, with the help of a pulley and geared motor, when a liquid film adhered to the substrate. The substrate together with the liquid film adhering to it was immediately transfered to a high temperature furnace for baking, where the chemicals reacted to form the desired solid film. Films are smooth, uniform and homogenious. X-ray diffractometric study suggests that, MoS_2 films deposited by the dip technique at a baking temperture of 300° C are amorphous in nature but those deposited at a higher baking temperatue of 360° C and 450°C are hexagonal in structure The optical bandgap (1 80 eV) calculated from the absorption measurement is quite comparable with the other reported value